epl A Letters Journal Exploring the Frontiers of Physics

October 2018

EPL, **124** (2018) 18003 www.epljournal.org
doi: 10.1209/0295-5075/124/18003

# Long-range strain correlations in 3D quiescent glass forming liquids

Muhammad Hassani[1], Elias M. Zirdehi[1], Kris Kok[2], Peter Schall[2], Matthias Fuchs[3] and Fathollah Varnik[1(a)]

[1] *ICAMS, Ruhr-Universität Bochum - Universitätsstraße 150, 44780 Bochum, Germany*
[2] *Institute of Physics, University of Amsterdam - Science Park 904, 1098XH Amsterdam, The Netherlands*
[3] *Fachbereich Physik, Universität Konstanz - 78457 Konstanz, Germany*

received 3 July 2018; accepted in final form 2 October 2018
published online 5 November 2018

PACS 81.05.Kf – Glasses (including metallic glasses)
PACS 62.20.-x – Mechanical properties of solids
PACS 62.20.F- – Deformation and plasticity

**Abstract** – Recent two-dimensional computer simulations and experiments indicate that even supercooled liquids exhibit long-lived, long-range strain correlations expected only in solids. Here we investigate this issue in three dimensions via Newtonian molecular-dynamics simulations, by a generalized hydrodynamics approach, and by experiments on Brownian hard-sphere colloids. Both in the glassy state and in liquid regimes, strain correlations are predicted to decay with a $1/r^3$ power law, reminiscent of elastic fields around an inclusion. In contrast, the temporal evolution of the correlation amplitude is distinct in the liquid state, where it grows linearly with time, and in the glass, where it reaches a time-independent plateau. These predictions are assessed via molecular-dynamics simulations and experiments. In simple liquids, the size of the cooperative strain patterns is of the order of the distance traveled by (high-frequency) transverse sound prior to structural relaxation. This length is of the order of nanometers in a normal liquid and grows to macroscale upon approaching the glass transition.



**Introduction.** – The existence of a growing length scale upon approaching the glass transition has been the subject of intense studies (see, *e.g.*, [1,2] and references therein). While earlier works mostly addressed quiescent systems, an alternative perspective to study glassy behavior has emerged in the last decade with a focus on non-equilibrium response [3,4]. Under steady shear, glasses show evidence of long-range strain correlations, resulting from the elastic coupling of local shear transformation zones [5]. This leads to a strongly correlated strain pattern which resembles the Eshelby solution around a pre-sheared spherical inclusion in a homogeneous isotropic elastic medium [6–10]. Relevance of these correlations for shear banding is also discussed in the literature [7,11–15]. Interestingly, long-range Eshelby-type correlations of strain fluctuations have been reported in molecular-dynamics (MD) simulations of a quiescent supercooled liquid in two dimensions [16]. Evidence for a fourfold symmetry of strain correlations has also been found from experiments on a quiescent colloidal glass [17]. These observations have been recently rationalized within the mode coupling theory, predicting additionally the time dependence of the correlation amplitude both in the glassy phase and in the supercooled regime [18]. These predictions have been tested via two-dimensional Brownian dynamics simulations of hard discs and experiments on colloidal mono-layers [18].

These long-range spatial correlations should play an important role in understanding the divergence of the structural relaxation time from liquid to glass. Yet, despite the fact that dimensionality plays a major role in the elastic response of solids —Eshelby fields decay as $1/r^d$ with $d$ being the spatial dimension— a detailed quantitative study of this problem in three dimensions is still lacking (see, however, [17] for a first study in the glassy state). Moreover, previous theoretical work on strain correlations [18] has dealt with Brownian systems only. Here, the case of Newtonian dynamics is addressed in 3D via generalized hydrodynamics and the projection operator technique by Zwanzig and Mori [19]. Importantly, the theory does not

(a) E-mail: fathollah.varnik@rub.de (corresponding author)

make any use of mode-coupling-type approximations and is thus applicable both to the normal liquid and deeply supercooled states. Predictions of this theory are examined quantitatively via MD simulations. Experiments on Brownian hard-sphere particles support these observations, and allow prediction of the corresponding elastic length scale upon properly accounting for the solvent friction.

**Generalized hydrodynamics.** – The correlation of accumulated strains at positions separated by distance $\mathbf{r}$ is defined as

$$C_{\boldsymbol{\varepsilon}}(\mathbf{r},t) = \langle \boldsymbol{\varepsilon}(\mathbf{r}+\mathbf{r}_0, t+t_0)\boldsymbol{\varepsilon}(\mathbf{r}_0,t_0)\rangle, \tag{1}$$

where the strain field, $\boldsymbol{\varepsilon}(\mathbf{r},t)$, is accumulated over time $t$ and is obtained from the integral of the symmetrized velocity gradient tensor:

$$\boldsymbol{\varepsilon}(\mathbf{r},t) = \int_{t_0}^{t_0+t} \mathrm{d}t'\, \frac{1}{2}(\nabla\mathbf{v}(\mathbf{r},t') + (\nabla\mathbf{v}(\mathbf{r},t'))^{\top}), \tag{2}$$

where $\top$ here stands for the transpose operator. This relation rests on the identification of the velocity field as time derivative of the displacement field, $\dot{\mathbf{u}}_{\mathbf{q}} = \mathbf{v}_{\mathbf{q}}$, and the familiar (linearized) relation between displacement and strain field. In an equilibrated and homogeneous system, the correlation $C_{\boldsymbol{\varepsilon}}$ does not depend on the arbitrarily chosen $\mathbf{r}_0$ and $t_0$. To compute $C_{\boldsymbol{\varepsilon}}$ and simplify the analysis, we apply a Fourier-Laplace transformation according to $C_{\boldsymbol{\varepsilon}}(\mathbf{q},s) = \int_0^\infty \mathrm{d}t \int \mathrm{d}\mathbf{r} e^{i\mathbf{q}\cdot\mathbf{r}-st} C_{\boldsymbol{\varepsilon}}(\mathbf{r},t)$. The advantage is that the transform $C_{\boldsymbol{\varepsilon}}(\mathbf{q},s)$ is directly related to the autocorrelation tensor of the velocity field, which is related to memory kernels in the Zwanzig-Mori approach. This approach uses the Fourier-Laplace space to perform the long-wavelength analysis of (generalized) hydrodynamics, which will be our basis for establishing the strain correlations in the far field [20]. The Zwanzig-Mori decomposition applied to $\mathrm{C}_{\boldsymbol{\varepsilon}}(\mathbf{q},s)$ gives the following result for a shear element [18]:

$$C_{\varepsilon_{xz}}(\mathbf{q},s) = \left(\frac{q_x^2+q_z^2}{4} - \frac{q_x^2 q_z^2}{q^2}\right)\frac{2}{s^2}K_q^{\perp}(s) + \left(\frac{q_x^2 q_z^2}{q^2}\right)\frac{2}{s^2}K_q^{\parallel}(s). \tag{3}$$

Here $\mathbf{K} = \langle \mathbf{v}_{\mathbf{q}}^*(t)\mathbf{v}_{\mathbf{q}}\rangle$ is the auto-correlation tensor of the velocity field, and superscripts indicate its two parts, longitudinal ($^{\parallel}$) and transverse ($^{\perp}$). These are connected to memory kernels $\mathbf{G}$ via

$$K_q^{(i)}(s) = \frac{v_{\mathrm{th}}^2}{s + \frac{q^2}{\rho}\left[\frac{\delta_{i\parallel}}{s\kappa_q^T} + G_q^{(i)}(s)\right]}, \tag{4}$$

which again arise from longitudinal or transverse fluctuations [20]. Here $\rho$ denotes the mass density and $v_{\mathrm{th}} = \sqrt{k_B T/m}$ the thermal velocity of particles with mass $m$. The Kronecker $\delta$ states that the $q$-dependent isothermal compressibility $\kappa_q^T$ only affects $K^{\parallel}$. The fluctuating force memory kernels $G_q^{(i)}(s)$ generalize the shear and longitudinal viscosity to finite frequencies and wave vectors. It is the law of momentum conservation which causes the appearance of hydrodynamic poles in $\mathbf{K}$ in eq. (4). They capture transverse momentum diffusion and longitudinal compressional waves in the long-wavelength and low-frequency limit of standard hydrodynamics, where the kernels can be replaced by transport coefficients (*viz.* viscosities).

The consequences of the obtained relations for strain correlations in liquids can be discussed within a simple model. In order to encode the growth of the viscosity when approaching the glass transition, a simple ansatz following Maxwell can be made for the transversal memory kernel [21]: $\mathrm{G}_q^{\perp}(t) \approx G^M(t) = G_\infty^{\perp} e^{-t/\tau}$ which should be valid for small wave vectors. Here $G_\infty^{\perp}$ is the macroscopic static shear modulus measurable in rheological spectra at intermediate frequencies $1/\tau \ll \omega \ll 1/\tau_0$ (with $\tau_0$ some microscopic time scale), and $\tau$ is Maxwell's relaxation time. The growth of $\tau$ explains the increase of the viscosity, $\eta = G_\infty^{\perp}\tau$.

Considering the system as incompressible and thus neglecting the longitudinal contribution to eq. (3) for the time being, one notices that the strain correlations obey a scaling law (in $d$ dimensions):

$$C_{\varepsilon_{xz}}(\mathbf{r},t) = \frac{1}{\xi^d}\left(\frac{v_{\mathrm{th}}}{v_{\mathrm{s}}}\right)^2 \tilde{C}_{\varepsilon_{xz}}(\mathbf{r}/\xi, t/\tau), \quad \text{where } \xi = v_{\mathrm{s}}\tau, \tag{5}$$

with a universal function $\tilde{C}_{\varepsilon_{xz}}(\tilde{\mathbf{r}},\tilde{t})$. Here the velocity $v_{\mathrm{s}} = \sqrt{G_\infty^{\perp}/\rho}$ of (high-frequency) transverse sound was introduced. Anticipating that the length $\xi$ becomes large in the considered supercooled fluids due to the rapid growth of the relaxation time $\tau$, the limit of $\xi \to \infty$ can be taken. It immediately predicts the appearance of spatial power law correlations in the far field, $C_{\boldsymbol{\varepsilon}_{xz}} \propto r^{-d}$. To be precise, for distances large compared to microscopic lengths but shorter than the size of the elastic domain, $a \ll r \ll \xi$, the transverse part reads

$$\tilde{C}_{xz}^{\perp}(\tilde{\mathbf{r}},\tilde{t}) = \frac{3}{8\pi}\frac{\tilde{J}^M(\tilde{t})}{\tilde{r}^3}\,\frac{\tilde{r}^2(\tilde{x}^2+\tilde{z}^2) - 10\tilde{x}^2\tilde{z}^2}{\tilde{r}^4}. \tag{6}$$

The spatial dependence follows Eshelby's far-field pattern of strain in an isotropic elastic solid (*e.g.*, in the plane $y=0$, a fourfold angular pattern results from the dependence on $x^2z^2$) [6]. The long-range pattern is built up by the diffusion of transverse momentum, which enters a factor $K^{\perp} \propto 1/(q\xi)^2$ in eq. (4) for small frequencies. Yet, because of the bigness of $\tau$, the temporal evolution still contains the fluid limit additionally to the expected solid limit. Both are contained in the (scaled) creep compliance $\tilde{J}$, which is the solution of $\int_0^{\tilde{t}} \tilde{G}(\tilde{t}-\tilde{t}')\tilde{J}(\tilde{t}')\mathrm{d}\tilde{t}' = \tilde{t}$, where $\tilde{G} = G_0^{\perp}/G_\infty^{\perp}$, in the general case. The compliance corresponding to Maxwell's ansatz for the modulus reads $\tilde{J}^M(t/\tau) = 1 + \frac{t}{\tau}$. For times short compared to the relaxation time, the pattern is constant as expected for a solid, which is described as state with $\tau = \infty$ according

to Maxwell. Only in fluid states, where $\tau$ is finite, also the limit $t \gg \tau$ can be accessed, where the strain keeps its spatial correlations but grows linearly with time. The overall prefactor then contains the viscosity.

In compressible systems, also longitudinal velocity fluctuations contribute to the shear strain in eq. (3). The correlation function then can be written as the sum of transverse and longitudinal contributions $\tilde{C}_{xz}(\tilde{\mathbf{r}},\tilde{t}) = \tilde{C}^{\perp}_{xz}(\tilde{\mathbf{r}},\tilde{t}) + \tilde{C}^{\parallel}_{xz}(\tilde{\mathbf{r}},\tilde{t})$, where the contribution of longitudinal velocity correlations to the far field reads

$$\tilde{C}^{\parallel}_{xz}(\tilde{\mathbf{r}},\tilde{t}) \to \frac{3}{8\pi}\,\frac{g^{\perp}\,\tilde{J}^{\parallel}(\tilde{t})}{\tilde{r}^3}\,\frac{10\tilde{x}^2\tilde{z}^2}{\tilde{r}^4}, \quad \text{for } \xi \to \infty. \quad (7)$$

Here, $g^{\perp}$ compares the frozen-in (macroscopic, *viz.* $\mathbf{q}=0$) shear modulus, $G^{\perp}_{\infty} = G^{\perp}_0(t\to\infty)$, to the isothermal compressibility, *viz.* $g^{\perp} = \kappa_0^T G^{\perp}_{\infty}$. This combination arises because the longitudinal velocity correlations are bounded by the fluid compressibility $\kappa_q^T$ and because of the factor $(v_{\rm th}/v_{\rm s})^2$, which is chosen as prefactor in the scaling law, eq. (5); it contains $1/G^{\perp}_{\infty}$.

The longitudinal compliance function $\tilde{J}^{\parallel}$ takes an explicit form when entering again a Maxwell ansatz for the longitudinal kernel with, for simplicity, the same relaxation time $\tau$ as in the transverse modes. The function $\tilde{J}^{\parallel}$ is not universal but depends on a parameter $g^{\parallel}$ which compares the frozen-in, macroscopic longitudinal modulus, $G^{\parallel}_{\infty} = G^{\parallel}_0(t\to\infty)$, to the isothermal compressibility, *viz.* $g^{\parallel} = 1 + \kappa_0^T G^{\parallel}_{\infty}$. The result in Laplace space reads $\tilde{J}^{\parallel}(\tilde{s}) = \tau(1+\tilde{s})/(\tilde{s}(1+\tilde{s}) + (g^{\parallel}-1)\tilde{s}^2)$. It only contributes appreciably to the strain pattern of the solid, where $\tilde{J}^{\parallel}(\tilde{t}\to 0) = 1/g^{\parallel}$, while it becomes negligible in the fluid state, where it remains bounded, $\tilde{J}^{\parallel}(\tilde{t}\to\infty) = 1$, whereas the transverse part grows linearly in time.

**MD simulation model.** – We use the standard Kob-Andersen model [22]. The simulation box is a cube with $L = 100$, containing 1.2 million particles ($\rho = 1.2$; all quantities are given in reduced LJ units). The mode coupling critical temperature of the model is $T_{\rm c} = 0.435$ [23]. Simulations are performed using LAMMPS [24] with a time step of $\mathrm{d}t = 0.005$. The model has been investigated in previous works, addressing various issues such as non-Newtonian rheology [25,26], heterogeneous plastic deformation and flow [15,27] and structural relaxation under shear [25,28]. Even though a crystalline equilibrium state exists for this model [29,30], the time necessary for crystallization exceeds by orders of magnitude the time window relevant for the present study. Periodic boundary conditions are applied along all the three spatial directions. No deformation or stress is applied to the system so that only inherent thermal fluctuations contribute to the strain.

**Experiments.** – To measure strain correlations in an experimental system, we use hard-sphere colloidal suspensions that are good model systems for glasses. In these systems, structural relaxations slow down significantly at volume fractions in the range 0.58–0.6, after which the glass can no longer equilibrate on experimental time scales [31]. We use sterically stabilized fluorescent polymethylmethacrylate (PMMA) particles with a diameter of $a = 2R = 1.47\,\mu$m and a polydispersity of 6% to prevent crystallization, suspended in a density and refractive-index matching mixture of cyclohexyl bromide and cis-decalin. Care was taken to meticulously balance the solvent composition to achieve the best density match after particles had swollen to their final size. To screen any possible residual charges, we also added a small amount of the organic salt TBAB (tetrabuthyl ammonium bromide). Suspensions at volume fractions of $\phi = 0.32$, 0.56 and 0.6 were then prepared by diluting samples quenched to a sediment, assuming a volume fraction of the sediment of 64%; the quench was achieved by changing the temperature to 29 °C, above room temperature, where due to differences in thermal expansion the particles become slightly heavier than the solvent. We image individual particles in three dimensions using confocal microscopy, and determine their positions with an accuracy of 40 nm in the vertical, and 20 nm in the horizontal direction using an iterative tracking algorithm. Each image covers a volume of $66\times100\times66\,(\mu\mathrm{m})^3 \approx 45\times68\times45a^3$, containing roughly 155000 colloids at the highest packing fraction investigated. Three-dimensional image stacks were acquired every minute over a time interval of 20 minutes. Particle positions were then linked between frames into particle trajectories, which were subsequently used to compute the local strain and strain correlations.

**Strain fluctuations and correlations thereof.** – Spontaneous strain fluctuations are evaluated via $\boldsymbol{\varepsilon}(\mathbf{r},t) = (\nabla\mathbf{u}^{\rm CG}(\mathbf{r},t) + (\nabla\mathbf{u}^{\rm CG}(\mathbf{r},t))^{\top})/2$, where $\mathbf{u}^{\rm CG}$ is a coarse-grained version of the displacement vector $\mathbf{u}_i(t) = \mathbf{r}_i(t+t_0) - \mathbf{r}_i(t_0)$ [10,32] ($i$ is a particle index). We have explicitly checked that coarse-graining does not bias the correlation function but only reduces the noise level (data not shown). Focusing on, say, the $xz$-component of the strain tensor, spatial correlations are evaluated via eq. (1) within thin slabs parallel to the $xz$-plane, $\mathbf{r} = r(\cos(\theta),0,\sin(\theta))$ with $\theta$ being the polar angle. To keep the dependence on radial distance only, we introduce,

$$C^4_4(r,t) = \frac{1}{\pi}\int_0^{2\pi} C_{\varepsilon_{xz}}(\mathbf{r},t)\cos(4\theta)\mathrm{d}\theta, \quad (8)$$

$$= \frac{C_s(t)}{r^3}. \quad (9)$$

In writing the second line above, eq. (9), we have made use of the $1/r^3$-scaling behavior of the strain-strain correlation function for $a \ll r \ll \xi$. A straightforward asymptotic analysis of $\tilde{J}_M(\tilde{t})$ and $J^{\parallel}(\tilde{t})$ appearing in eqs. (6) and (7), respectively, leads to the following prediction for the correlation amplitude:

$$C_s(t) = \begin{cases} \dfrac{15\rho k_{\rm B}T}{32\pi m}\left(\dfrac{1}{G^{\perp}_{\infty}} - \dfrac{1}{G^{\parallel}_{\infty}}\right), & \text{glass,} \\ \dfrac{15\rho k_{\rm B}T}{32\pi m}\,\dfrac{t}{\eta}, & \text{liquid.} \end{cases} \quad (10)$$

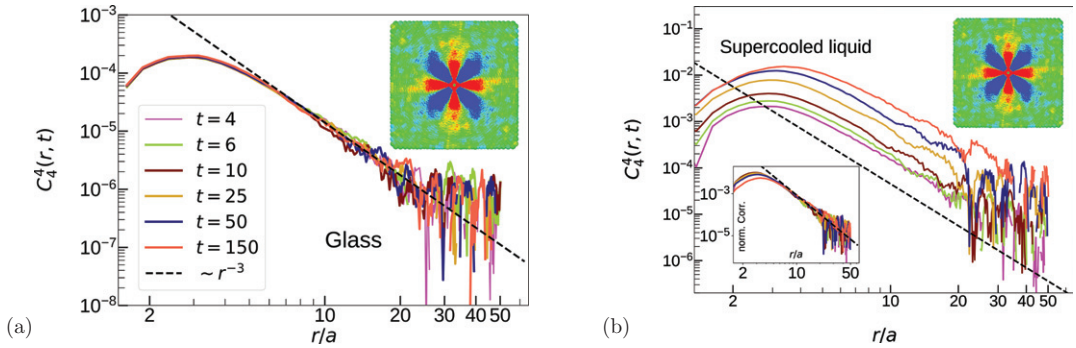


Fig. 1: (Color online) Correlations of strain fluctuations obtained from MD simulations of a generic binary LJ glass former at temperatures of (a) $T = 0.2$ (glassy state) and (b) $T = 0.7$ (supercooled liquid). The curve legends in (a) apply to both panels and give the time, $t$, over which strain is accumulated, eq. (2). Both in the glass and in the (supercooled) liquid, the correlation function decays with a power law $1/r^3$ at distances large compared to a particle diameter. The amplitude of the correlation function, however, is constant in the glass but continuously grows in the liquid state. The upper right insets show color scale plots of the correlation function, highlighting the fourfold symmetry. The lower left inset in (b) shows the same data divided by $C_s(t)$, eq. (10).

Here, the longitudinal contribution in the compressible glass is included.

These predictions are obtained for a Newtonian system. It is well known that the microscopic dynamics has little influence on the structural dynamics at the glass transition [33]. This is recovered by the theoretical predictions here and in ref. [18], with an important difference to be discussed below after first examining the strain correlations by both Newtonian simulations and experiments on Brownian hard-sphere colloids.

**Results.** – MD results on the correlation function of shear strain fluctuations are shown in fig. 1 both for the glassy state ($T = 0.2$) (recall that $T_g \approx 0.4$ [26]) and in the (supercooled) liquid. As seen from the inset, strain correlations exhibit quadrupolar symmetry. This observation is in qualitative agreement with previous two-dimensional simulations [16] and experiments [17]. To investigate the spatial dependence of the correlations in more detail, we project them onto the corresponding circular harmonic given by $\cos(4\theta)$, eq. (8), and study their radial decay.

In the glass (fig. 1(a)) and for all the times $t$ used to evaluate the accumulated strain, the (non-normalized!) correlation functions obey a master curve with a power-law decay, $1/r^3$, for distances large compared to the particle size. This is the domain relevant for continuum mechanics, where effects arising from molecular scale structure become irrelevant. It is interesting to compare this behavior of a glass to that of a (supercooled) liquid (fig. 1(b)). In this case, the strain correlation still obeys a power law with exponent $-3$ but the amplitude of correlations increases with time.

A quantitative analysis of the correlation amplitude, $C_s(t)$, is depicted in fig. 2. No fit parameter is used for this comparison with eq. (10). Rather, all the constants are evaluated from independent simulation studies. Both in the glass and in the (supercooled) liquid states, simulation results agree well with the theoretical predictions.

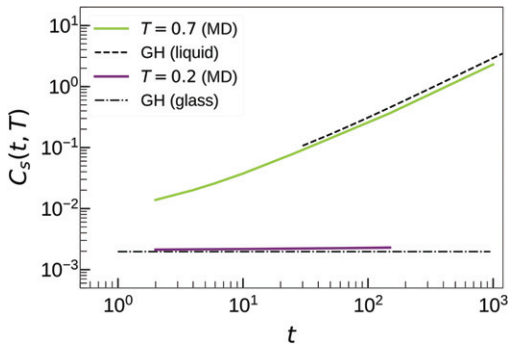


Fig. 2: (Color online) The correlation amplitude *vs.* time at temperatures of $T = 0.7$ (supercooled liquid state) and $T = 0.2$ (glass). The dashed lines give theoretical predictions within generalized hydrodynamics (GH) for the respective cases, eq. (10) ($\rho = 1.2$, $k_B = 1$, $G_\infty^\perp(T = 0.2) = 15$ [34], $G_\infty^\parallel(T = 0.2) = 86.3$, $\eta(T = 0.7) = 42$).

A qualitatively similar trend is observed in experiments on polydisperse colloidal hard spheres (fig. 3). We again observe a quadrupolar symmetry as in simulations. Moreover, the projected correlation functions decay with the same power of $-3$ *vs.* radial distance, irrespective of the volume fraction and the time interval, over which the strains are computed. While the power-law decay is thus robust over the volume fractions from fluid to dense glass, the correlation amplitude varies, showing different trends for fluid and glass. This is shown in fig. 3(b), where we plot the correlation magnitude at the origin ($r = 0$) as a function of observation time interval for the three volume fractions. With increasing time $t$, the lowest volume fraction shows a growth of correlation amplitude, approaching a power of $\sim$1 towards the end; thus, in line with theory and MD simulations, the correlation amplitude grows with the amount of strain accumulated during the observation time interval. In contrast, the higher volume fractions show only a shallow increase of correlations, indicating a

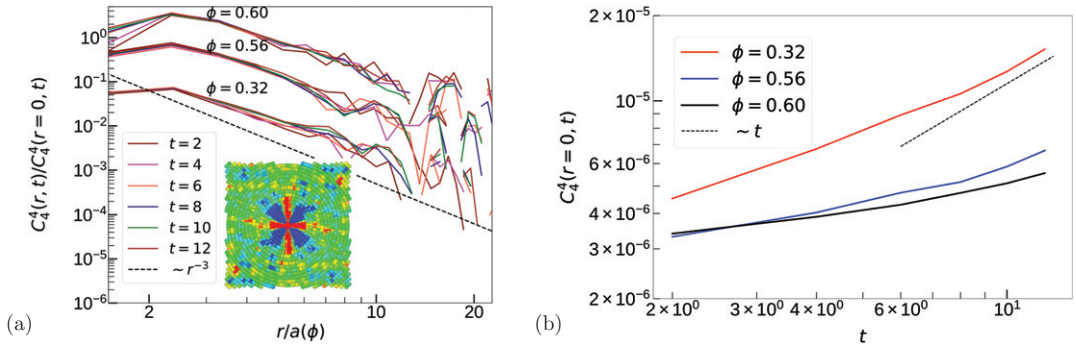


Fig. 3: (Color online) Experimental results on normalized correlations of strain fluctuations in a hard-sphere colloidal glass former. Panel (a) shows the correlation function *vs.* in-plane distance, $r/a(\phi)$, after integration over the polar angle, eq. (8). Here, $a(\phi)$ is the average inter-particle distance, obtained from the first minimum of the radial pair distribution function. The data are presented for three volume fractions of $\phi = 0.32$, 0.56 and 0.60. Strain correlations are computed over time intervals of $t = 2, 6, 8, 10$ and 12 min. For all three volume fractions, the data show approximately a power-law decay with an exponent of $-3$. In (b), the amplitude of the correlations for the three volume fraction is shown. It exhibits a quasi-plateau close to and at the glassy state ($\phi = 0.56$ and $\phi = 0.6$), while it grows linearly in the fluid regime ($\phi = 0.32$). The inset in (a) shows a color scale plot of the correlation function for $\phi = 0.32$, highlighting the fourfold symmetry.

quasi-plateau at small time intervals. These trends, which agree qualitatively with the predictions in eq. (10), are confirmed in other experimental data sets of quiescent colloidal glasses over similar ranges of volume fraction (data not shown).

**Size of elastic domains in the liquid state.** – For a Newtonian system, the length scale associated with a solid-like response in the liquid state is predicted to be given by $\xi \sim \tau\sqrt{G_\infty^\perp/\rho}$, where $\tau$ is a structural relaxation time, and $G_\infty^\perp$ the high-frequency shear modulus. Recalling that the speed of transverse sound waves is given by $v_\mathrm{s} = \sqrt{G_\infty^\perp/\rho}$, it is seen that $\xi \sim \tau v_\mathrm{s}$ [21]. Using this relation, the fourfold pattern and the characteristic $1/r^3$ decay of spatial correlations finds a simple interpretation. A local shear deformation event generates a signal which propagates with the speed of sound in the surrounding medium. As long as no structural relaxation takes place during the propagation of the signal, the region "visited" by the signal appears as an elastic medium. This ceases to be the case as time exceeds the structural relaxation time. It is noteworthy that the idea of a "solid-like" region in a liquid has been around for a while. Dyre, for example, predicted that the size, $l$, of such a region scales as $l \sim (v_\mathrm{glass}\tau)^{1/4}$, where $v_\mathrm{glass}$ is the longitudinal sound velocity in the glass and $\tau$ is the time between two "flow events" in a sphere of radius $l$ [35]. However, transverse collective hydrodynamic modes, which preserve momentum and which give rise to long-range correlations, were not considered there.

A correlation length, which is closely tied to —and linearly grows with— the structural relaxation time has also been reported in the case of a four-point dynamic structure factor, constructed from the full complex self-intermediate scattering function [36,37]. Interestingly, the increase of the correlation length is attributed to the growth of transient elastic response. A growing length has also been observed in the related crossover from diffusion to wave propagation in the transverse momentum correlations [38]. Recently, it was shown that it also determines the far-field stress correlations [21].

In a typical liquid, the speed of sound is of the order of 1000 m/s. Using $\tau \sim 10\,\mathrm{ps} = 10^{-11}\,\mathrm{s}$ for the structural relaxation time, one thus obtains $\xi \sim 10^{-8}\,\mathrm{m} = 10\,\mathrm{nm}$, corresponding already to 10–50 molecular diameters. In the glassy state, $\tau \sim 100\,\mathrm{s}$, which yields $\xi \sim 1000\,\mathrm{m}$, a truly macroscopic length scale. To estimate $\xi$ for our simulations, we have performed a thorough analysis of the stress autocorrelation function in the quiescent system and the frequency-dependent elastic modulus under oscillatory shear. As a result of these investigations whose details will be reported elsewhere, we have determined $G_\infty^\perp$ and $\tau$ for the present binary LJ model both in the (supercooled) liquid state and in the glass. We find $G_\infty^\perp \approx 13$ and $\tau \approx 3$ in the liquid ($T = 0.7$), which gives $\xi \approx 10$. Interestingly, this estimate is quite close to the one obtained from the Maxwell approximation for the stress relaxation time, $\tau = \eta/G_\infty^\perp$, which leads to $\xi = \eta/\sqrt{\rho G_\infty^\perp}$ and thus $\xi \approx 11$, where $\eta(T = 0.7) = 42$ was used. In the glassy state ($T = 0.2$), the shear modulus raises only slightly ($G_\infty^\perp \approx 16$) but the relaxation time grows by orders of magnitude, $\tau \geq 10^5$, leading to $\xi(T = 0.2) \geq 10^5$, far beyond the simulation box size.

The fact that, depending on temperature, the size of the elastic domain in the supercooled state can be of the order ten particle diameters is encouraging to study a possible crossover from the long-range Eshelby-like quadrupolar correlations to a different behavior, characteristic of the liquid state. The present set of data, however, does not show a clear signature of such a crossover. We shall here recall that the above estimate of the length scale $\xi = \tau v_\mathrm{s}$ is based on a scaling argument and thus contains an *a priori*

unknown numerical factor. Future studies with larger simulation box sizes could help to elucidate this issue.

To estimate $\xi$ for the experiments, we have to take a different route as the description of the overdamped colloidal system differs in one respect from a liquid governed by Newtonian dynamics. Here, forces on the particles arise also from the solvent. These forces can be considered rapid and fluctuating, but violate conservation of the colloid particles' momentum because the solvent on average exerts friction. Modeling the colloidal particles by Langevin equations [39], the memory kernels in eq. (4) are replaced by $q^2 G_q^{(i)}(s)/\rho \to \frac{\zeta}{m} + q^2 G_q^{(i)}(s)/\rho$. Here, $\zeta$ can (for simplicity) be taken as Stokes friction coefficient. Considering the overdamped limit, where friction dominates over inertia, $\zeta \gg ms$, the strain fields can be estimated for colloidal dispersions. The strain patterns described in eqs. (6) and (7) keep their form, yet the expression for the correlation length changes to $\xi^2 = G_\infty^\perp/(n\zeta_0)\tau$ [18], where $n$ is the particle density. Apparently, signals from deformation events now propagate by a random walk with diffusion coefficient given by elastic relative to viscous forces. We estimate the corresponding correlation length $\xi$ from measurement of the shear modulus taken from [40], and relaxation time taken from [41]. In the volume-fraction regime from $\phi = 0.32$ to 0.6 investigated here, the shear modulus changes from some $100 k_B T/R^3$ to $\sim 2000 k_B T/R^3$, while the glass relaxation time changes from $\sim 10\tau_0$ to the values above $10^6\tau_0$, where $\tau_0$ is the relaxation time at infinite dilution defined by $\tau_0 = R^2/(6D_0)$ with the diffusion coefficient $D_0\zeta_0 = k_B T$. Using these values, one finds that the length $\xi$ increases from $\xi/R \sim 36$ at $\phi = 0.32$ to $\xi/R \sim 2500$ at $\phi = 0.56$ and to $\xi/R \gtrsim 37000$ at $\phi = 0.6$. This indicates that the crossover to the fluid regime may be outside the accessible length scale range, even at the lowest volume fraction studied ($\phi = 0.32$). Indeed the strain correlations in fig. 3(a) show an $r^{-3}$ decay over the full range, without clear signature of a finite correlation length.

**Conclusion.** – In this work, we investigated correlations of strain fluctuations in quiescent glasses and supercooled liquids via experiments and computer simulations in three dimensions. Both in the glassy state and in the supercooled liquid, experimental and simulated strain correlations decay with a $1/r^3$ power-law decay, reminiscent of Eshelby's pattern. The fourfold symmetry is also preserved in both cases investigated. The spatial pattern arises from diffusive transport of transverse momentum coupled into the strain field. The difference between the glassy and liquid states manifests itself in the time dependence of the correlation amplitude which forms a plateau in the glassy state whereas it grows linearly in the supercooled liquid state. Qualitatively, the strain amplitude follows a Maxwellian compliance in response to thermal stresses. All these observations are rationalized within a generalized hydrodynamic theory, applied here to the present 3D problem. The length scale associated with the size of solid-like response in the supercooled regime is given by the distance traveled by transverse sound waves during the structural relaxation time. In overdamped systems, it is the distance over which the elastic forces diffuse during the time $\tau$. It ranges from tens of nanometers in the high-temperature normal liquid state to macroscopic lengths of the order of a kilometer in the glassy state. From this follows that accompanying the dramatic increase of the relaxation time, there is indeed a strongly increasing correlation length scale, namely that of the elastic-like quadrupolar response of the material. A thorough study of this length and its implication for spontaneous strain correlations upon approaching the glass transition remains an interesting challenge for future work.

* * *

Financial support by the German Research Foundation (DFG) under the grant number VA 205/18-1 is acknowledged.

REFERENCES

[1] Bennemann C., Donati C., Baschnagel J. and Glotzer S. C., *Nature*, **399** (1999) 246.
[2] Karmakar S., Dasgupta C. and Sastry S., *Rep. Prog. Phys.*, **79** (2016) 016601.
[3] Berthier L., Barrat J.-L. and Kurchan J., *Phys. Rev. E*, **61** (2000) 5464.
[4] Fuchs M. and Cates M. E., *Phys. Rev. Lett.*, **89** (2002) 248304.
[5] Falk M. L. and Langer J. S., *Phys. Rev. E*, **57** (1998) 7192.
[6] Picard G., Ajdari A., Lequeux F. and Bocquet L., *Eur. Phys. J. E*, **15** (2004) 371.
[7] Chikkadi V., Wegdam G., Bonn D., Nienhuis B. and Schall P., *Phys. Rev. Lett.*, **107** (2011) 198303.
[8] Nicolas A., Rottler J. and Barrat J.-L., *Eur. Phys. J. E*, **37** (2014) 50.
[9] Talamali M., Petäjä V., Vandembroucq D. and Roux S., *C. R. Méc.*, **340** (2012) 275.
[10] Hassani M., Engels P. and Varnik F., *EPL*, **121** (2018) 18005.
[11] Dasgupta R., Gendelman O., Mishra P., Procaccia I. and Shor C. A. B. Z., *Phys. Rev. E*, **88** (2013) 032401.
[12] Chikkadi V., Mandal S., Nienhuis B., Raabe D., Varnik F. and Schall P., *EPL*, **100** (2012) 56001.
[13] Mandal S., Chikkadi V., Nienhuis B., Raabe D., Schall P. and Varnik F., *Phys. Rev. E*, **88** (2013) 022129.
[14] Chikkadi V., Miedema D. M., Dang M. T., Nienhuis B. and Schall P., *Phys. Rev. Lett.*, **113** (2014) 208301.
[15] Hassani M., Engels P., Raabe D. and Varnik F., *J. Stat. Mech.: Theory Exp.*, **2016** (2016) 084006.
[16] Chattoraj J. and Lemaitre A., *Phys. Rev. Lett.*, **111** (2013) 066001.
[17] Jensen K. E., Weitz D. A. and Spaepen F., *Phys. Rev. E*, **90** (2014) 042305.
[18] Illing B., Fritschi S., Hajnal D., Klix C., Keim P. and Fuchs M., *Phys. Rev. Lett.*, **117** (2016) 208002.
[19] Zwanzig R. and Mountain R. D., *J. Chem. Phys.*, **43** (1965) 4464.

[20] Hansen J.-P. and McDonald I. R., *Theory of Simple Liquids* (Academic Press, London) 1990.
[21] Maier M., Zippelius A. and Fuchs M., *Phys. Rev. Lett.*, **119** (2017) 265701.
[22] Kob W. and Andersen H. C., *Phys. Rev. Lett.*, **73** (1994) 1376.
[23] Kob W. and Andersen H. C., *Phys. Rev. E*, **52** (1995) 4134.
[24] Plimpton S., *J. Comput. Phys.*, **117** (1995) 1.
[25] Berthier L. and Barrat J.-L., *J. Chem. Phys.*, **116** (2002) 6228.
[26] Varnik F. and Henrich O., *Phys. Rev. B*, **73** (2006) 174209.
[27] Varnik F., Bocquet L., Barrat J.-L. and Berthier L., *Phys. Rev. Lett.*, **90** (2003) 095702.
[28] Varnik F., *J. Chem. Phys.*, **125** (2006) 164514.
[29] Pedersen U. R., Schrøder T. B. and Dyre J. C., *Phys. Rev. Lett.*, **120** (2018) 165501.
[30] Ingebrigtsen T. S., Dyre J. C., Schrøder T. B. and Royall C. P., *Crystallisation instability in glassforming mixtures*, arXiv:1804.01378v1 [cond-mat.soft].
[31] van Megen W. and Underwood S. M., *Phys. Rev. E*, **49** (1994) 4206.
[32] Goldenberg C., Tanguy A. and Barrat J.-L., *EPL*, **80** (2007) 16003.
[33] Gleim T., Kob W. and Binder K., *Phys. Rev. Lett.*, **81** (1998) 4404.
[34] Varnik F., Bocquet L. and Barrat J.-L., *J. Chem. Phys.*, **120** (2004) 2788.
[35] Dyre J. C., *Phys. Rev. E*, **59** (1999) 2458.
[36] Flenner E. and Szamel G., *J. Phys. Chem. B*, **119** (2015) 9188.
[37] Flenner E. and Szamel G., *J. Phys.: Condens. Matter*, **27** (2015) 194125.
[38] Torchinsky D. H., Johnson J. A. and Nelson K. A., *J. Chem. Phys.*, **136** (2012) 174509.
[39] Hess W. and Klein R., *Adv. Phys.*, **32** (1983) 173.
[40] van der Vaart K., Rahmani Y., Zargar R., Hu Z., Bonn D. and Schall P., *J. Rheol.*, **57** (2013) 1195.
[41] van Megen W. T. C., Mortensen S. R. W. and Müller J., *Phys. Rev. E*, **58** (1998) 6073.